Wader

the international journal of shorebird science

Study

Tracking the full annual-cycle of the Great Knot *Calidris tenuirostris*, a long-distance migratory shorebird of the East Asian-Australasian Flyway

Simeon Lisovski[1,2], Ken Gosbell[3], Chris Hassell[4] & Clive Minton[5]

[1]*University of California, Department of Neurobiology Physiology and Behavior, Davis, CA 95616, USA.*
simeon.lisovski@gmail.com
[2]*Deakin University, School of Life and Environmental Science, Centre for Integrative Ecology, VIC 3220 Geelong, Australia*
[3]*1/19 Baldwin Road, Blackburn, VIC 3130, Australia*
[4]*Global Flyway Network, Po Box 2089, Broome, WA 6725, Australia*
[5]*165 Dalgetty Rd, Beaumaris, VIC 3193, Australia*

The Great Knot *Calidris tenuirostris* is one of the iconic long-distance migratory species of the East Asian-Australasian Flyway. However, despite extensive flagging and banding efforts, very little is known about the migratory strategies and the breeding grounds of this species that spends the non-breeding season mainly on the northern shorelines of Australia. Using light-level geolocators deployed on Great Knots at Roebuck Bay (Western Australia), we describe the individual migration strategies, breeding locations and breeding-related behaviour. Based on data from eight successfully tracked individuals, we found that all except one migrated to the western part of the known breeding range. This was 2,000–2,500 km from the eighth individual that commenced breeding in the potentially separated eastern part of the range. Light intensity and temperature profiles provided evidence that four of the birds successfully hatched chicks. Of the three which failed, one appeared to have laid a second clutch before failing again. Arrival at the breeding grounds and the laying of eggs were remarkably synchronous between individuals, as were the arrival dates back at Roebuck Bay. Departure from the breeding grounds was more spread out, partly dependent on breeding success and also as a result of females probably leaving the nesting area before males. The individual migration strategies confirmed the strong dependence of this species on the Yellow Sea as their major stopover site during both southward and northward migration. Furthermore, all individuals stopped at least once on their northward journey to the Yellow Sea from Australia. And in reverse, all individuals stopped at least once on the southward migration before arriving at the Yellow Sea coming from their Arctic breeding grounds. The results indicate that this species will most likely be further affected by the rapid habitat loss in the area of the Yellow Sea and other parts of the Chinese coastline.

Keywords

Arctic-breeding waders

breeding success

light-level geolocation

migration

stopover ecology

Yellow Sea

INTRODUCTION

The Great Knot *Calidris tenuirostris* is the iconic species for the huge increase in the knowledge of waders in the East Asian-Australasian Flyway over the last few decades. As late as 1980 it was thought to be an 'uncommon' species in Australia (Lane 1987). However, this picture changed dramatically in 1981 when Australasian Wader Studies Group (AWSG) expeditions and surveys along the coasts of northern Australia found flocks numbering tens of thousands of Great Knots, particularly in Roebuck Bay at Broome and along Eighty Mile Beach (Lane 1987). We now know that there are almost 425,000 individuals (Hansen *et al.* 2016) that migrate from their Siberian breeding sites to the coastlines of Australia and southern Asia (Lane 1987, Lappo et al. 2012). However, recent

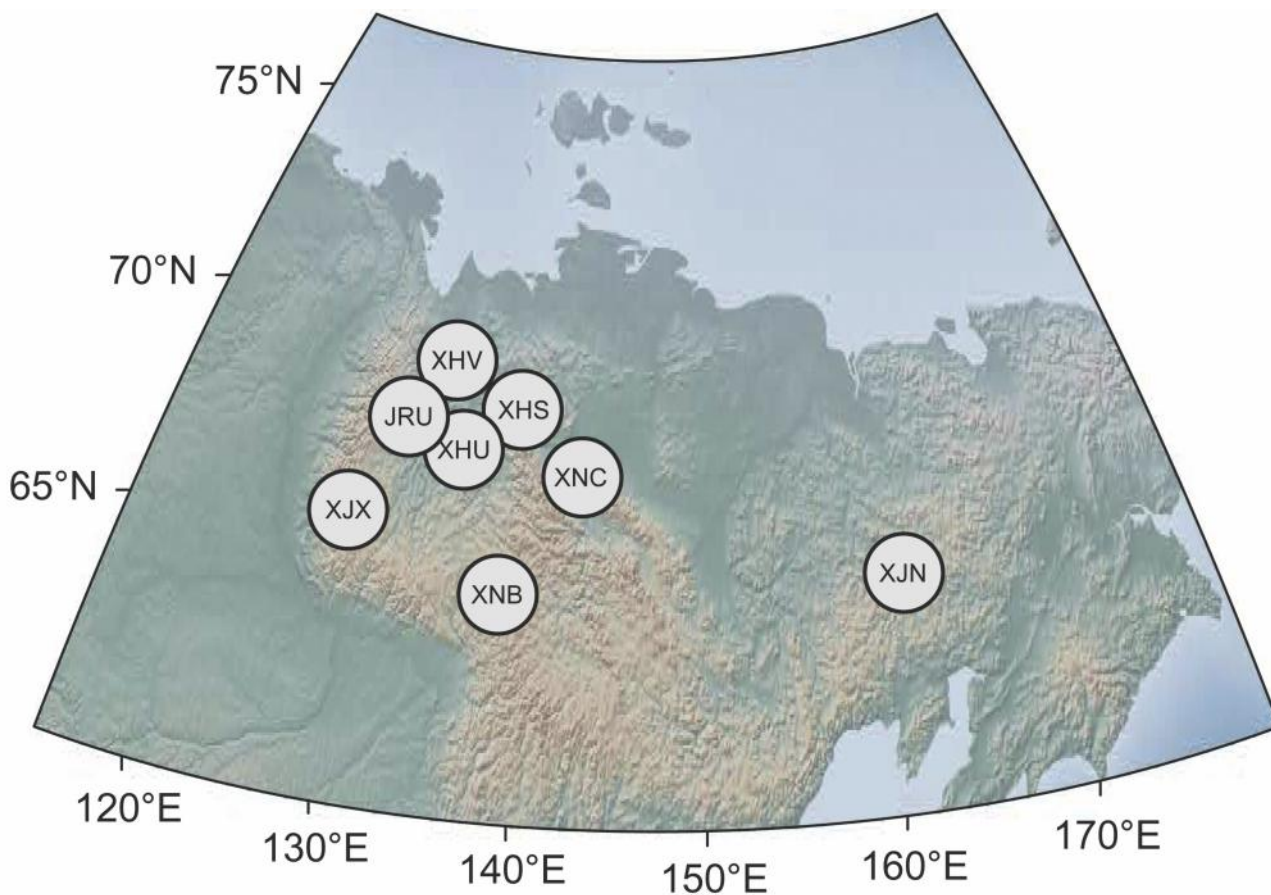**Fig. 1.** Estimated breeding sites of individual Great Knots spending the non-breeding season in north-west Australia. Location estimates are based on a template fit method using light-level geolocator data (see Lisovski *et al.* 2016). The known breeding range is restricted to the sub-alpine zone of the mountain ranges (light brown areas; Lappo *et al.* 2012). Labels refer to engraved flag codes of the individual Great Knots.

analyses showed that numbers were likely even higher just a few decades ago (Rogers *et al.* 2007, Clemens *et al.* 2016). The large-scale loss and degradation of important refuelling habitat along their migratory journey, and notably the Yellow Sea (Ma *et al.* 2014, Murray *et al.* 2014) is widely thought to be driving decreases in migratory shorebirds in general and Great Knot populations in particular (Piersma *et al.* 2016). Complete ground counts of the entire length of Eighty Mile Beach revealed a 20% reduction of numbers over ~10 years (Rogers *et al.* 2007). A continent-wide analysis showed a similar number of ~1.8% population decline per year (Clemens *et al.* 2016).

The Great Knot was also one of the first species providing evidence that migrating waders from Australia could perform very long non-stop flights; in the mid 1980s, hunters at Chongming Dao, in the mouth of the Yangtze River near Shanghai in China, were regularly catching banded birds, occasionally as little as 7–12 days after they had been originally marked at Broome and 80 Mile Beach (AWSG banding data). Furthermore, even though the Great Knot is the one of the most abundant shorebirds in Australia, nowhere in south-east Asia does it occur in

large numbers during the migration periods (Higgins & Davies 1996). This suggested a potential non-stop-flight of 5,500 km which was considered an almost unbelievable achievement at that time. We now know that many Charadriiformes, and notably Arctic-breeding wader species, commence their journey northwards with a long and fast migratory flight of up to 8,500 km for Far Eastern Curlew *Numenius madagascariensis* (Minton *et al.* 2013) and about 10,000 km for Bar-tailed godwits *Limosa lapponica baueri* (Battley *et al.* 2012).

Despite the significant increase in knowledge about Great Knots and the fact that around 33,500 individuals have been banded and flagged in Australia, very little is known about their breeding areas in Siberia. The few flag resightings – birds leg-flagged in north-west Australia (Minton *et al.* 2011) and in Chukotka, Russia (Tomkovich 2003) – involve the area east of the Kolyma Highlands at the north-eastern end of the expected breeding range in Siberia (Tomkovich 1997). Furthermore, two banding recoveries indicate movements between the same areas – the Anadyr region and Roebuck Bay near Broome in north-west Australia (AWSG banding data). However, considerable information has been gathered through recoveries and flag

sightings *en route*, together with populations counts (Barter *et al.* 1997). These data indicate the great importance of the Yellow Sea as a key stopover location on northward and southward migration (Tomkovich 1997, Minton *et al.* 2011). The Great Knot was thus one of the first species shown to be critically dependent on the Yellow Sea. There has also been a steady trickle of recoveries, mainly from hunters, and flag sightings, from the southern shores of the Sea of Okhotsk in July/August each year suggesting that this might be another major stopover location during southward migration (Huettmann 2001, 2003, AWSG flag resighting database). With reports of large numbers of waders seen on radar flying southwards over the Sea of Japan (Williams & Williams 1988) and relatively lower numbers of Great Knots in the Yellow Sea during southward migration (Barter 2002), it was even speculated that some Great Knots might be flying straight back to the north coast of Australia from that area.

The objective of the present study was to track the full annual cycle of individual Great Knots using light-level geolocators. We here aim to reveal information on individual movements independent of the potential bias of flag resightings, which are dependent on the presence of observers (see Lisovski *et al.* 2016). The geolocator tracking data will thus allow us to evaluate and discuss the previously gathered information from banding and flagging activities. Furthermore, we aim to make use of the slight changes in light intensities at the breeding sites with 24 hours daylight to estimate the breeding location of each bird and draw inferences on incubation and chick rearing behaviour using light patterns and temperature recordings of the tags (Burger *et al.* 2012, Gosbell *et al.* 2012).

METHODS

Capture and tracking data

Great Knots were captured in cannon nets at high tide roosts on the northern beaches of Roebuck Bay, Broome, in north-west Australia (122.22°E, 17.97°S). A total of 57 geolocators (Intigeo-W65, Migrate Technology Ltd, Cambridge, UK) were deployed between 26 February and 12 March 2013. The units were mounted on plastic leg-flags (made from a Darvic PVC sheet) using Kevlar thread reinforced with Araldite resin cement. The geolocator units weighed 0.65 g and when mounted on a flag the combined weight was 1.2 g. This represents less than 1% of the typical fat-free weight of 140 g for Great Knots in north-west Australia. All except for one unit were deployed on adult birds considered to be in their third year of life (or older). Ageing was based on plumage; at that time of year adult Great Knots have extensive breeding plumage with heavy black spotting on the upper breast and extensive rufous-brown and black colouring on the upper parts. During the subsequent non-breeding period following deployment, Great Knots carrying geolocators were specifically targeted in cannon net catches. Morphometric measurements were available for only three of the tracked individuals and were used to determine their sex; a prob-

ability of being a male or a female was assigned to those individuals using a discriminant function analysis (lda function in R; Venables & Ripley 2002) based on morphometric measurements (bill length, head length and wing length) of 33 Great Knots with known sex (P.S. Tomkovich & M.Y. Soloviev unpubl. data).

Geolocator analysis

Light intensity recordings from geolocators were used to estimate the breeding sites of each individual and the incubation pattern. Subsequently, using the derived breeding site position, the full migration path was estimated. Great Knots are known to breed at latitudes above 60°N (Lappo *et al.* 2012) and thus experience constant daylight during this part of their annual cycle. Conventional methods to estimate positions from light intensity recordings over time and defined sunrise/sunset times (i.e. threshold method in light-level geolocation) fail to produce position estimates under 24-h daylight conditions as the light does not fall below the horizon and sunrise/sunset times cannot be detected (Lisovski *et al.* 2012). We used the *template fit analysis* described by Lisovski *et al.* (2016) to estimate the positions of the breeding site. In short, the method evaluates the possibility that the observed variation in light intensities during 24-h daylight could have been recorded at locations within a given boundary (100–180°E and 55–85°N). We selected the lowest latitudinal position with the possibility value of 100%. For more details, code and explanations see Lisovski *et al.* (2016).

Both the light intensity recordings and the recorded temperature patterns over time can be used to make inferences of the incubation and chick rearing behaviour on the breeding grounds. With regard to the light pattern, we used a similar method as described by Gosbell *et al.* (2012) in which the occurrence of alternating 'light' and 'dark' signals in the geolocator output recorded in the breeding area was interpreted as an indication for shading associated with nesting activities including especially incubation and brooding. We defined light intensities as 'dark' or 'light' if they fell below or above the 15% quantile of all light intensity measurements during the breeding period. We then calculated the daily percentage of 'darkness'. We interpreted alternating high and low daily percentage of 'darkness', expected to occur due to the alternating incubation efforts between partners (Tomkovich 1997), as incubation. Extended periods of elevated but constant daily percentage of 'darkness' after a period of potentially successful incubation of approx. 20–24 days (Tomkovich 1997), were interpreted as chick-brooding activity. The minimum temperature recordings calculated and stored on the geolocators every four hours were used to refine the interpretation of the dark-light patterns. Since the geolocator devices are attached to the leg, the temperature recordings during incubation are expected to be significantly higher than expected ambient temperatures at Arctic breeding sites. The minimum temperature recordings were used since they were expected to indicate the difference between extended periods of incubation (high minimum tempera-

tures) and non-incubation (low minimum temperatures). Similarly to the dark-light pattern, we interpreted alternating patterns of low and high minimum temperatures as incubation and periods of elevated minimum temperatures after potentially successful incubation as chick-brooding activity.

To evaluate the migratory pathways for each individual, two daily locations were estimated from raw light-level data using the simple threshold method with a light intensity threshold of 0.8 to define sunrise and sunset times (Lisovski *et al.* 2012). The required zenith angle was derived from on-bird calibration data recorded at a known location prior to or after migration. To further improve the location-estimation accuracy, we used a Bayesian framework that incorporated prior knowledge of Great Knot behaviour and provided location estimates with associated measurements of uncertainty. This step was done using the R-package 'SGAT' (Wotherspoon *et al.* 2013), which employs Markov Chain Monte Carlo (MCMC) simulations that permit a *spatial probability mask*, prior definition of the error distribution of twilight events (*twilight model*), and plausible flying speed values (*behavioural model*). For a detailed description of model assumptions see Sumner *et al.* (2009) and Lisovski *et al.* (2016). The *spatial probability mask* was based on the premise that Great Knots are most commonly found along the coast during migration. Estimated positions were therefore considered to be 4 times more likely if close to the coast and increasingly less likely with increasing distance (d, in meters) from the shore using [$1 + 3*exp(-(d/50000)^3)$] (resulting in values between 4, close to the coast, and 1 at large distance from the coast). The *spatial probability mask* was based on a shoreline dataset with a 1:75,000 scale (NOAA Shoreline Website). To parameterize the *twilight model* a log-normal density distribution was fitted to the calibration data (i.e. light intensity recordings from known location). The density distribution was fitted to the difference (twilight error) of the zenith angle of each twilight time recorded during the calibration period and the first/last recorded sunrise/sunset time, assuming that the latter set of twilight times was recorded without any shading. The parameters log-mean and log-sd of the individually fitted log-normal density distribution were then used to describe the *twilight model*. For the *behavioural model* we assumed that Great Knots perform stepwise migrations, with relatively long staging periods in between periods of movement (Piersma 1987, Warnock 2010). We modelled flight (ground) speed using a gamma distribution (shape = 0.7, scale = 0.05) assuming that the speed with the highest probability was below one (i.e. the bird is most likely to be stationary at any given time) and that a maximum average flying speed measured between two positions of up to 80 km/h was possible during migration (Pennycuick *et al.* 2013). For each individual we used these parameters and all available information in the MCMC simulation to create 'samples', each sample reflecting one full set of positions connecting each twilight event along the entire migration path from non-breeding to breeding grounds. We started by drawing an initial 10,000 samples for burn-in and tuning of the spatial probability distribution of the individual. Next, a further 40,000 samples were drawn to visually evaluate convergence of the model. Finally, an additional 2,000 samples were drawn to generate the ultimate posterior distribution and the most likely migration path of each individual including its confidence range.

Movement patterns

To distinguish between periods of residency (i.e. fuelling, roosting and breeding) and periods of movement we used the 'changeLight' function from the R-package 'Geo-Light' (Lisovski & Hahn 2012). This analysis quantifies the probability of each sunrise and sunset to be different from the preceding and following sunrise and sunset times, hence providing probabilities for shifts in positions (henceforth referred to as changepoint probability). We used the median of the MCMC posterior distribution (i.e. the most likely migration path), to calculate the sunrise and sunset times for each estimated location. For each individual, we calculated the changepoint probability for each twilight time. Periods of residency were defined as the (maximum) time periods during which all twilight times had a changepoint probability lower than 0.8 for a minimum duration of two days. These are rather conservative parameter settings that often result in many spatial overlaps between periods of residency. We therefore subsequently used the 'mergeSite' function from the R-package 'GeoLight' to combine stationary periods, i.e. consecutive sites where the median positions are less than 500 km apart.

Migratory itineraries

While the MCMC simulation refines the spatial accuracy of the location estimates, it may have a negative effect on the temporal patterns: locations close to a shoreline and potentially close to subsequent defined stopover site will likely be pushed towards the shoreline, because of the mask, and towards the stopover site, because of the movement model. To enable maximum accuracy in the migratory itineraries, we used the so-called conductivity data recorded by the geolocator devices. This data source provides information on whether the logger device has been exposed to salt water or not and often reveals clear borders between stationary periods and periods of dry conditions during flight. We used the exact start and end date of wet periods that co-occurred with stationary periods from location estimates (±1 d) and in this scenario with both methods confirming each other, we considered the timing as highly accurate. In case a wet period was not conclusive for an identified stationary period and due to lacking confidence in exact arrival and departure data, we did not include the surrounding flight bouts in the analysis of flight speed and duration. Processing scripts for location estimates (R code), raw light-level data, and processing results used in this study were uploaded onto Movebank (*http://movebank.org*; study name 'Tracking Great Knots along the EAAF').

RESULTS

Retrieval of geolocators

Twelve geolocators were retrieved during the two non-breeding seasons 2013/14 and 2014/15 following deployment. This corresponds to a retrieval rate of 21%, slightly above the long-term retrap rate of banded Great Knots in north-west Australia (13%). The higher retrap rate is most likely attributed to an increased effort in catching those individuals. However, this finding suggests no decrease in the survival probability of Great Knots carrying a geolocator. One geolocator failed prematurely and three birds, including the juvenile individual (XNR), did not migrate, resulting in eight complete annual tracks for analyses.

Breeding sites

Breeding sites could be estimated for all individuals (Fig. 1). All estimated locations were in the known breeding range of Great Knots in the subalpine zone of mountain ranges in the northern half of East Siberia, though away from the northern coast itself. However, while 7 of the 8 individuals were found in the western part of the known distribution, one individual (XJN) had a disjunct estimated breeding site at about 160°E towards the eastern end of the known distribution.

Incubation patterns

The analysis of the minimum temperature and 'light-dark' pattern recorded during the breeding period indicates that all individuals except XNB commenced incubating 8–12 days after arrival (Fig. 2a). In four individuals (XJN, XJX, XHU and XNC), the clear alternating 'light-dark' pattern and elevated temperatures continued long enough (22–24 d) to suggest that eggs successfully hatched. Individuals XHS, XHV, and JRU also showed evidence for clutch initiation and incubation, but aborted after a few days, indicating nesting failure. In JRU the incubation pattern lasted only for about 4 days. However, the minimum temperature data, not the 'light-dark' pattern, suggested that this individual initiated a second clutch approximately 10 days later and again aborted incubation after a few days. The very late-arriving bird, XNB, did not show any signs of breeding and departed from the area after only 13 days. Periods of potential chick-brooding were observed for XJN and possibly for XJX and XHU. The fourth individual with potential success in incubation (XNC) left the breeding site shortly after the chicks hatched (approx. 5–7 d). Incubation bouts varied from 4 to 20 hours with a general increase towards the end of the incubation period. An example of raw light and temperature recordings during the breeding period is shown in Fig. 2b,c. Detailed graphs on minimum temperature patterns for each individual can be found in supplementary material S1.

Migration routes and schedules

All eight individuals performed a complete northward migration from the deployment site in Roebuck Bay to their breeding grounds and back (Fig. 3). The mean distance between wintering and breeding site was 9,561 km (SD ± 182 km), resulting in a mean round trip of 19,122 km. The geolocator of one individual (XHU) stopped recording during the first half of its southward migration. Conductivity data and location estimates indicated stopover sites and were almost always in agreement. The exception was at a few short stopover sites where conductivity data were inconclusive (see supplementary material S2).

Northward migration. Most Great Knots departed from Roebuck Bay between 26 March and 6 April. One (XJN) left a little later, on 26 April, but XNB did not leave until 30 May, long after the normal migration season. Generally, all individuals used a similar route with a fast migration leg from Roebuck Bay to the coastline of China. Six individuals had one or two very short (2–8 d) stops during this first major leg. All but one individual had their major staging site within the area of the Yellow Sea, six in China and one in North Korea. XJX however did not stop within this region and had its major stopover site in the area of Taiwan. Individuals spent 10–41 days (median: 34 d) or 40–69% (median: 59%) of their entire northward migration in the Yellow Sea (XJX not included in this statistic). After their major stopover all individuals flew straight to their breeding sites where they arrived during 18–26 May. XNB however did not arrive until 25 June. Ignoring the latter individual, all other tracked Great Knots reached their breeding sites over a period of 8 days. Northward migration, on average, was completed in 46.5 days, with a maximum of 57 days (XHV) and a minimum of 25 days in the late-departing individual XJN. All individuals spent at least twice as much time on the ground at stopover sites as they did actually flying during the northward migration. Mean total speed of migration was 224.2 km/d during northward migration, with ground speeds between 24 and 92 km/h (great circle distance between stopover sites).

Southward migration. All tracked individuals departed their breeding locations between 27 June and 25 July. One logger (XHU) failed to record light intensities shortly after the departure. In contrast to the northward migration, all individuals had at least one stopover – mostly south-west Sea of Okhotsk – between the breeding sites and their major stopover location, which was again in the Yellow Sea. Individuals spent 12–41 days (median: 23 d) or 26–61% (median: 47%) of their entire southward migration in the Yellow Sea (XHU not included in this statistic). From there, three individuals flew straight to Roebuck Bay, whereas the other four individuals had one very short additional stopover on an island of south east Asia (e.g. Philippines). All tracked Great Knots arrived at Roebuck Bay between 23 August and 6 September. The 'late' bird XNB arrived back on 6 September, having remained in the Yellow Sea until 1 September. Southward migration, on average, was completed within 54 days, with a maximum of 68.5 days (XHS) and a minimum of 44 days (XJX). Except for XNC all individuals spent considerably more time and also relatively more compared
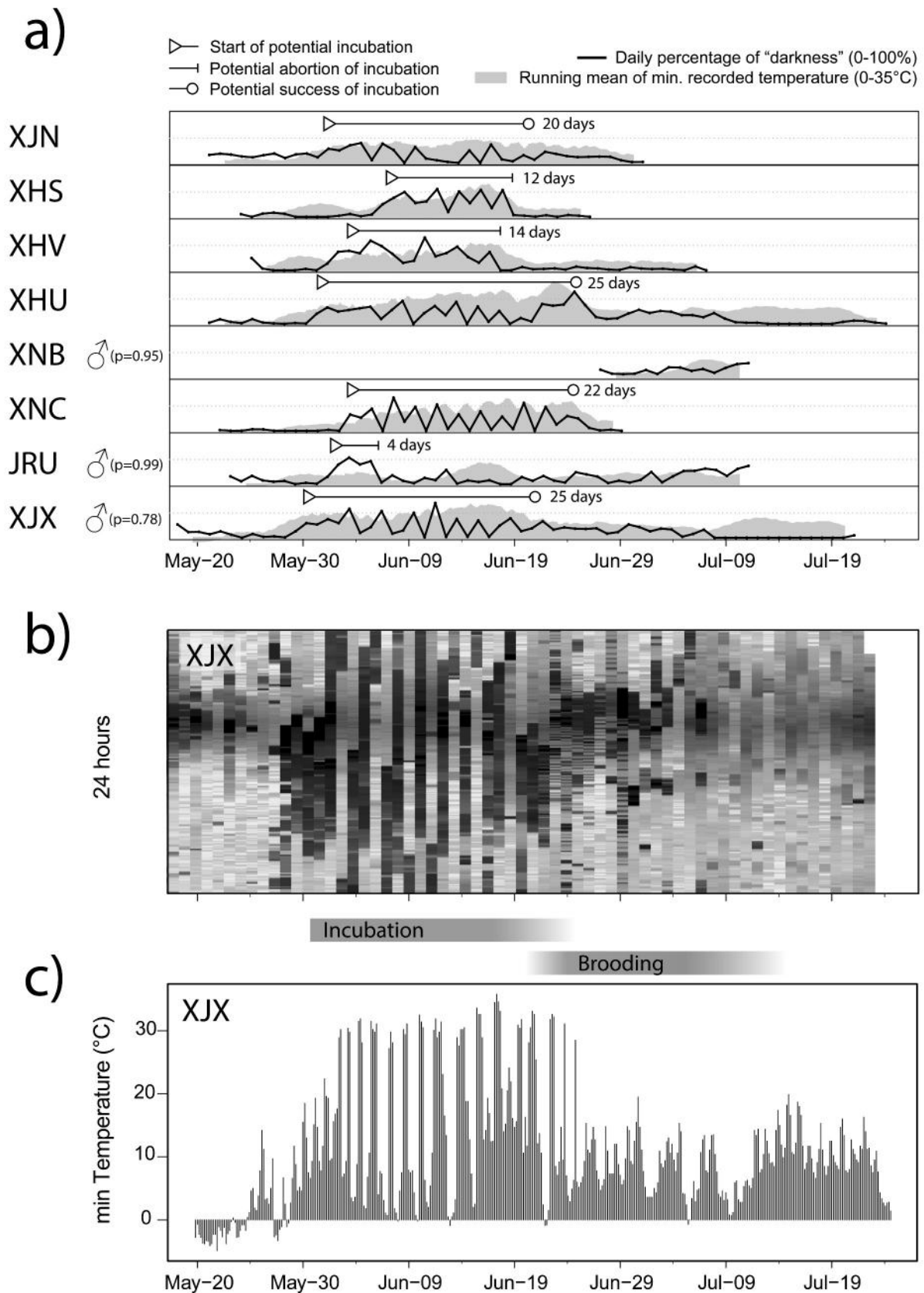
Fig. 2. (a) Individual incubation activity interpreted from 'dark-light' and minimum temperature output of the geolocators. Black lines indicate the daily percentage of 'darkness' (bird sitting on its legs) and grey areas indicate the mean minimum temperate over time. Both time series start and end with the individual arrival and the departure from the breeding site. Potential start, end and abortion of incubation is shown above the 'dark-light' and minimum temperature pattern. Information on the sex of the individual is based on a discriminant analysis and values indicate the probability of belonging to the indicated sex based on morphometric measurement (bill length, head length and wing length). Example of raw light intensity measurement **(b)** and minimum temperature **(c)** recordings of XJX.

to northward migration, on the ground at stopover locations than in actual flight. Mean total speed of southward migration was 179 km/d, with ground speeds of 13–74 km/h (see S2 for more details).

DISCUSSION

In this study, we successfully followed eight individual migrations of Great Knots from their non-breeding sites in north-west Australia to their breeding grounds in the sub-alpine transition zone of Arctic and boreal habitats in eastern Russia. Light-level geolocators were used not only to infer migration routes and breeding sites but also to investigate breeding patterns and the potential success of incubation.

Tracking birds with light-level geolocators has become a frequently used technique in migratory research and has led to many new and exciting discoveries. In recent years, both the hardware and the analytical techniques required to derive location estimates from the raw light intensity data have made major advancements. The results of this study demonstrate once again the huge potential of this tracking technique to study the full-annual cycle of a long-distant migratory bird. However, light-level geolocators remain an indirect tracking technique that uses light, a measure that is almost never unaffected by some sort of shading like clouds, to estimate locations (see Lisovski *et al.* 2012). We must realise that location estimates from even the most advanced tags and most sophisticated software are still subject to some level of uncertainty. Here, we provide locations of stopover sites and estimates of breeding sites. While we expect the estimated stopover locations to be quite accurate, given the strong preference of Great Knots to the shoreline (during migration) and the absence of strong shading through e.g. vegetation, the results should be interpreted without making a very strong inference on the exact locations. Even more caution is needed when it comes to the breeding site estimates. Light intensities at those locations and during the summer change only very little over time and any shading has a strong effect. Yet, we can use the results to investigate major spatial patterns in the breeding distribution between the individuals. But the reader should not be disappointed, if planning to go out into the field and find the nest based on those data, that they need to be prepared to at least look into the 200–400 km vicinity.

The largely frugivorous breeding diet of Great Knots seems to restrict the northern limit (70°N) of the species distribution to the sub-alpine mountain ranges with regular crops of berries (Lappo *et al.* 2012). This restriction may have led to two rather disjunct breeding ranges, one in the Kolyma Highlands and eastwards to the Pacific Ocean where one of the tracked individuals (XJN) has been located. The western breeding range is located in the mountains of north-central Yakutia, the large area used by all other individuals (Fig. 1). The only existing leg-flag resightings of Great Knots from Australia at their breeding sites were two birds seen near Anadyr, at the eastern end of the breeding range, 2,300km east of the main group of geolocator birds. Our finding of two rather separate breeding ranges may support the previously suggested possibility of two biogeographic breeding populations that mix on the non-breeding grounds in Australia (Delany & Scott 2006).

With the exception of XNB, which departed very late from Australia resulting in an equally late arrival in the Arctic, all individuals arrived at the breeding grounds relatively synchronously between 18 and 26 of May (Fig. 3). Great Knots are known to be one of the earliest arrivals on the breeding grounds compared to other wader species (Tomkovich 1997) and the arrival dates here reported were similar to dates recorded for the closely-related Red Knot *C. canutus rogersi* (Loktionov *et al.* 2016). Incubation was initiated 8–12 days after arrival and lasted 3–24 days. Tomkovich (1997) suggests an incubation period of 22.5 days, after the last egg of the clutch has been laid, for successful hatching. Hence four of the tracked birds with incubation periods of 22–24 days were most likely successful while the remaining three with incubation durations of 3–16 days were judged to have failed due to e.g. predators, adverse weather conditions or some other unknown reason. The close match of the estimated incubation periods with the 22.5 days measured in the field (Tomkovich 1997) may indicate that our analysis identifies the approximate time of the laying of the last egg and the time when adults increase their incubating effort. Re-nesting has previously been shown for some wader species in the Arctic (Gosbell *et al.* 2012, Loktionov *et al.* 2016) but it is considered uncommon. It may be significant that the only Great Knot appearing to have re-laid eggs after an initial failure was the one which only lasted for four days originally.

Fig. 3 (overleaf). Northward (left globes) and southward (right globes) migration of individual Great Knots. The routes are presented as a series of consecutive stopover sites (resting and/or fuelling sites) connected by the shortest great circle distance route. The size of the stopover site (black circle) is scaled according to the stopover duration (3–30 d). The middle panel shows the latitudinal movement, based on the most likely path from the MCMC simulation, with the departure and arrival dates from the deployment site in north-west Australia and the breeding grounds. The bar charts indicate the days each individual was on the move or stationary (fuelling/resting) during northward and southward migration. Raw map data were downloaded from: *naturalearthdata.com*.
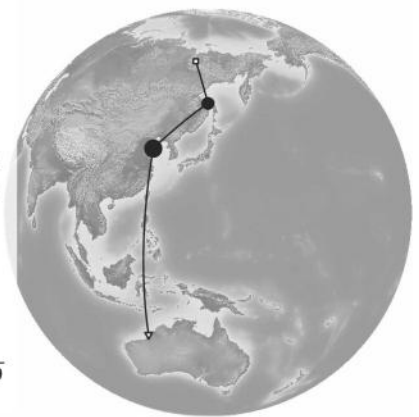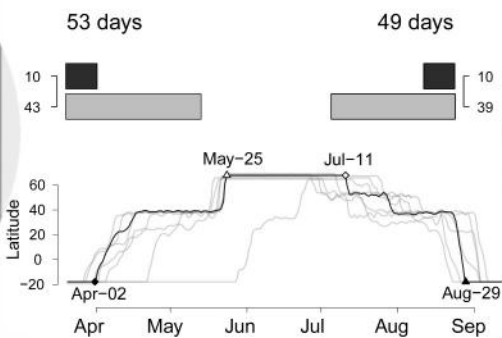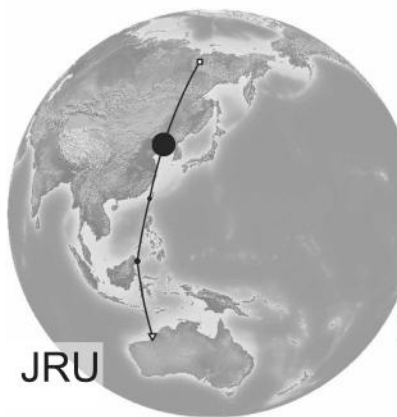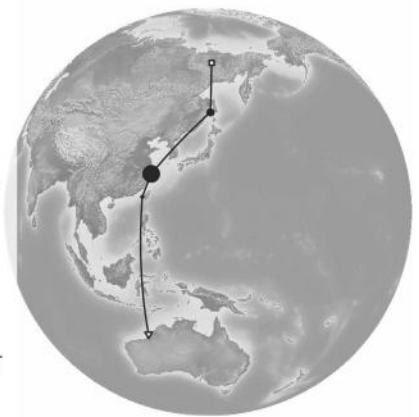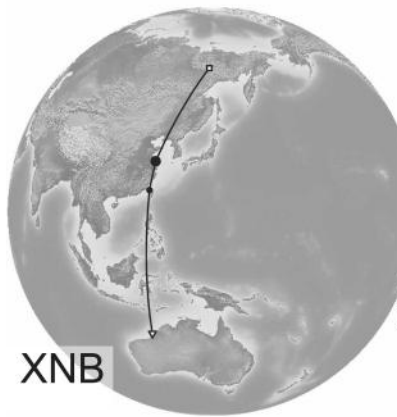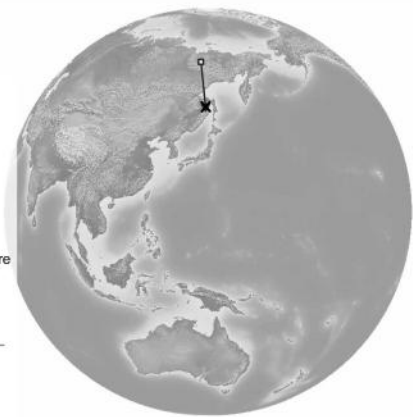
Northward Migration

Southward Migration
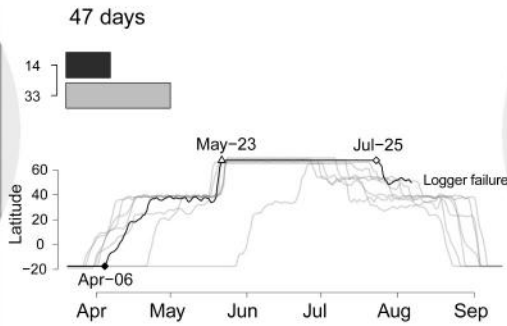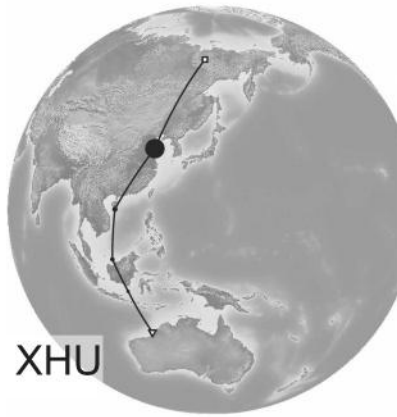
Northward Migration

Southward Migration

XHU

XNB

XNC

JRU
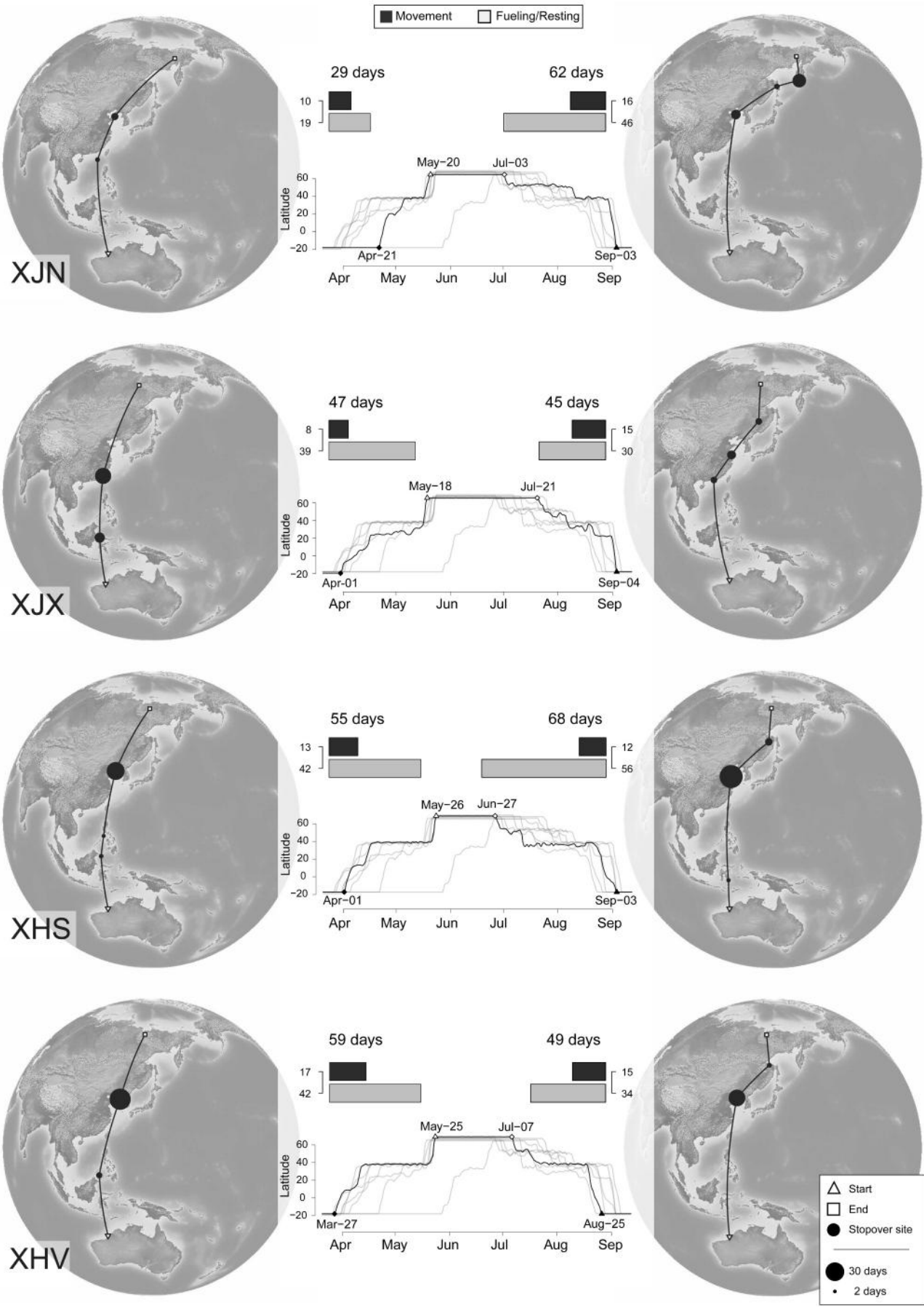
Northward Migration
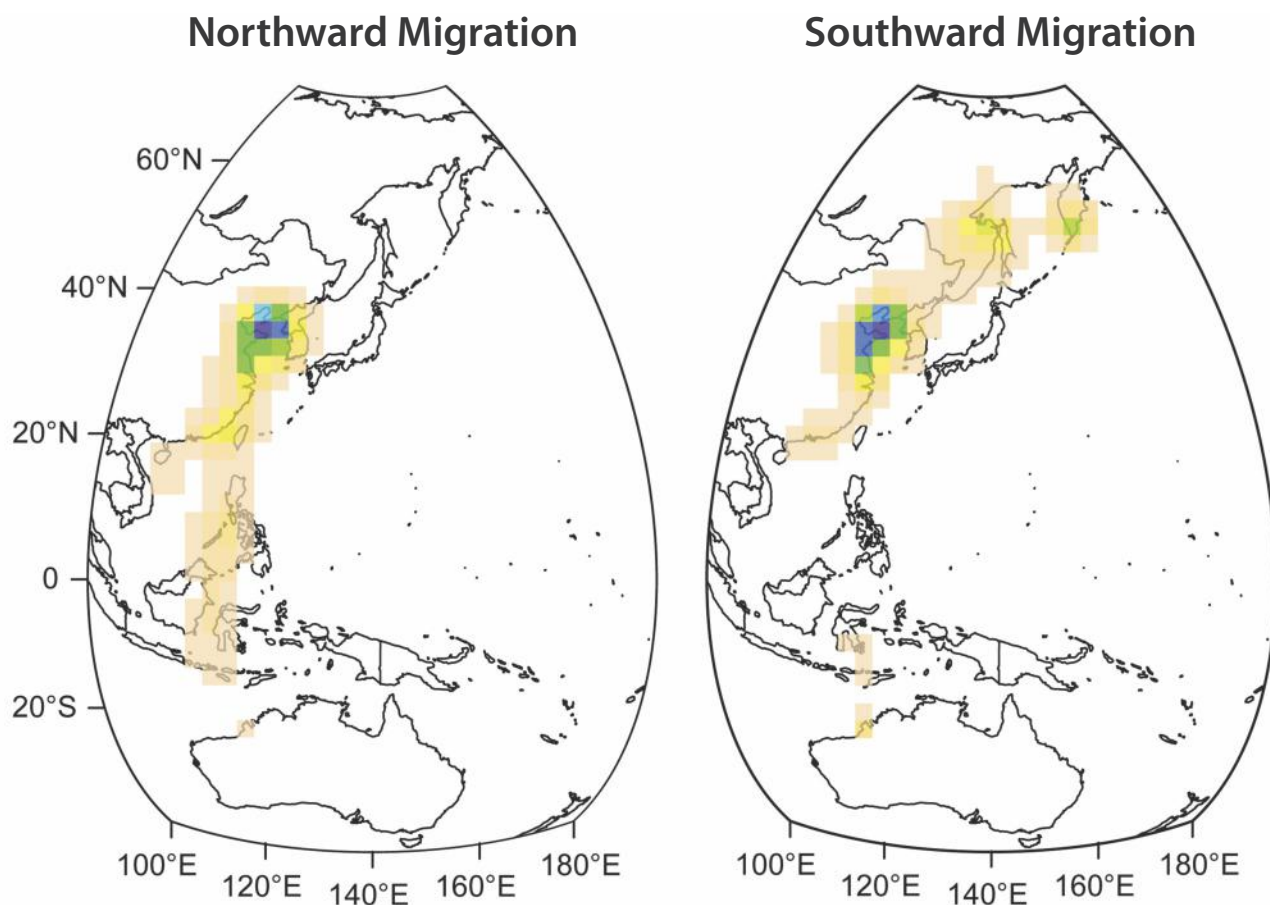
Southward Migration
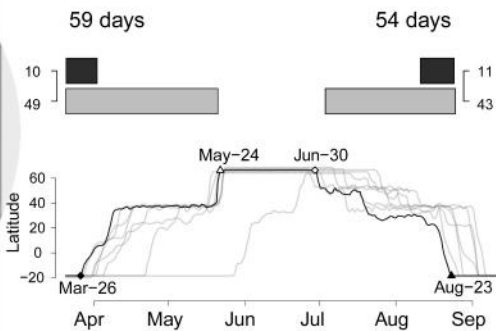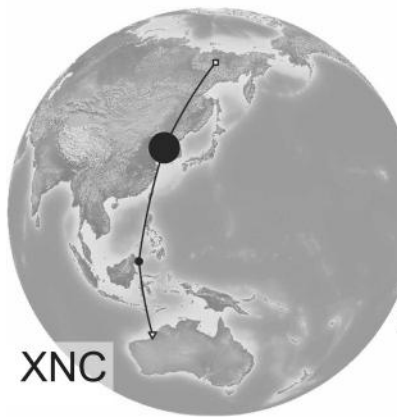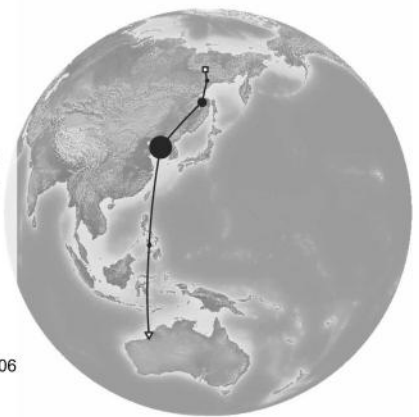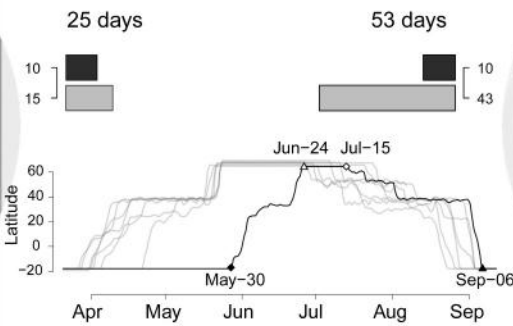
Fig. 4. Relative time spent (coloured squares) at stopover sites during northward (left) and southward (right) migration. The values represent the sum of all tracked individual Great Knots during periods when birds were stationary between the geolocator deployment site in north-west Australia and the breeding grounds.

However, the second attempt had an equally brief incubation period (Fig. 2 & S1). Incubation bouts varied from 4 to 20 hours, and an increase in length was observed as the incubation period progressed. Loktionov *et al.* (2016) noted a similar pattern including observing incubation bouts of up to 20 hours for Red Knot males in the latter part of the incubation period. This was a different pattern to that observed for Ruddy Turnstone (Gosbell *et al.* 2012) in which a parabolic relationship was shown with the longest bouts being recorded around the mid-term of incubation. This study again shows that light-level geolocators can provide detailed information on duration and timing of incubation behaviour. In addition, they also provide some indication of the extent to which parents brood their chicks after hatching. While the exact length of this activity is often difficult to resolve because of its irregularity due in part to climatic conditions, there is some evidence that the four birds with successful incubation brooded chicks for a certain period of time after the chicks hatched, indicated by high frequency of 'dark-light' transitions (see Fig. 2 & S1). However, brooding behavior is difficult to quantify and often not 100% conclusive. Loktionov *et al.* (2016) suggested that the period of incubation and/or brooding post-hatching might be used to indicate the sex of the birds. It is known that

female Red Knots (and several other species of Arctic-breeding waders) tend to leave the chicks and depart the breeding grounds before the males. Tomkovich (1997) reported similar behaviour in the Great Knot. In the current study bird XJX, known to be a male, departed the breeding grounds 30 days after hatching. As the interval for bird XHU was 31 days, it is likely also to be a male. Conversely, XNC and XJN which departed the area 5 and 12 days after hatching are likely to be females. However, the latter could alternatively have been males that departed after e.g. losing their chicks.

Importantly, our findings also provide further evidence that Great Knots use the Yellow Sea as the major stopover location on both northward and southward migration (Fig. 3 & 4). Interestingly, the geolocator location estimates provide evidence that all but one bird used the Chinese coast of the Yellow Sea for extended periods during their migration. Given that so much of the intertidal habitat there has been lost to land reclamation in recent years (Ma *et al.* 2014, Murray *et al.* 2014) it may not be surprising that Great Knot numbers in Australia have decreased markedly (Clemens *et al.* 2016) especially just after the huge Saemangeum project in South Korea was completed in 2007 (Moores *et al.* 2016). As a consequence,

the Great Knot's conservation status has recently been reclassified as Critically Endangered (The Environment Protection and Biodiversity Conservation Act, a.k.a. EPBC Act). Besides the Yellow Sea, Great Knots from Broome seem to make one other significant stopover on both northward and southward migration (Fig. 2). On the northward journey this was before the Yellow Sea stopover utilising the islands of south-east Asia, the central Chinese coast and Taiwan. On southward migration we found the reverse pattern with stopovers north of the Yellow sea in the Sea of Okhotsk. And while very little is known about the importance of stopover sites between Australia and the Chinese coastline, the Sea of Okhotsk is well known for large numbers of transient Great Knots (Gerasimov *et al.* 1999, Gerasimov & Gerasimov 2000, Huettmann 2001, Antonov & Huettman 2008). During northward migration, all individuals, except for XJN, either did not visit or spent only a very short period of time (<1.5 d) in the western part of the Sea of Okhotsk (Fig. 3 & S2). The easterly breeding individual XJN passed areas known to host large numbers of Great Knots during this particular time (~15–18 May; Tomkovich 1997, Huettmann 2001), however, our data suggested no stopovers in this area. We can only speculate, but our data suggest that during northward migration, the Sea of Okhotsk is most important for populations migrating to the eastern parts of the known breeding range. In contrast, during southward migration, Great Knots recorded in the western part of the Sea of Okhotsk including the northern Sakhalin Island may come from the entire breeding range. We found no evidence for a long onward movement from these areas directly to north-west Australia. All birds instead went south via the Yellow Sea.

Some interesting features were shown in the aberrant migratory behaviour of XNB (Fig. 2). It did not leave Broome until 30 May, by which time all the other Great Knots had started to lay eggs on their breeding sites. It made only a short stopover in the Yellow Sea (10 d) and so completed the total northward migration faster than any of the other Great Knots. Nevertheless, by the time it arrived on the breeding grounds (21 June) most of the other birds had either completed or aborted incubation. Not surprisingly it did not nest and it departed after only a short stay of about 15 days. It is not clear what delayed this bird in the first place and it raises the question of why it continued all the way up to the breeding grounds when the chance of breeding successfully must have been so slim. Aborting migration is a previously reported phenomenon in shorebird species. Lisovski *et al.* (2016) reported a Sanderling *Calidris alba* staying an extended period in south China before returning to the non-breeding site in Australia. In Great Knots it is reported that large numbers of non-breeding individuals spend the northern summer on the coast of the Sea of Okhotsk (Tomkovich 1997) or even skip migration and remain on the coastlines of Australia (AWSG database). In fact, many migratory wader species remain on the non-breeding grounds during their first calendar year (e.g. Summers *et al.* 1995) or in some cases achieve only parts of the migratory

distances (e.g. a one-year-old bird shot at Sakhalin Island; Tomkovich 2003). Thus it was no surprise that the one juvenile individual carrying a geolocator did not migrate. The reason for the other two individuals that omitted migration remains unknown. We are confident that these individuals, as well as the very late-departing XNC, were aged correctly and were at least in their second calendar year. The potential negative effect of handling the bird and deploying a geolocator can never be ruled out, although it seems unlikely (Weiser *et al.* 2016). It might also be possible that some adult individuals decide to not migrate for reasons such as infections or generally poor body condition.

A rather novel feature of the migratory journeys of Great Knots discussed here is that most birds stopped at least once, for 2–8 days at a time, after departing Roebuck Bay and before arriving at the Chinese coast (Fig. 3). Those short stays would have been too brief to have acted as a significant 'refuelling' stop and are thus considered as resting sites only (Ma *et al.* 2013). This finding obviously challenges the notion that almost all individuals commence their migratory journey with a ~5,000 km non-stop flight from Australia to the coastline of China (e.g. Battley *et al.* 2000). While flag resightings of Great Knots within 7 days from Roebuck Bay and the Yellow Sea as well as the rapid (~5 d) and non-stop initial migration bout of about 4,700 km of XNB certainly provides strong evidence for the potential for such non-stop long-distance flights, the low density of observers and the potential large spatial spread of resting individuals on the islands of south-east Asia and the southern coastline of China may have contributed to misconceptions about this migratory pattern. Interestingly, the pattern of short stopovers during northward migration to the Yellow Sea was repeated in the tracked Great Knots with observed short resting periods during southward migration before arriving at the Yellow Sea. After the long stopover on the coasts of the Yellow Sea or the southern Chinese coast, the individuals performed a rather fast and direct flight to their final destination. Apparent migration speeds varied widely between each migration leg. The range of over-ground speeds measured on some of the longer legs of the journey, and thus the legs where departure and arrival time could be estimated with high precision, was similar to those measured from geolocators on a range of other waders in the EAAF; i.e. 50 (SD ± 5) km/h (Minton *et al.* 2013).

In conclusion, the results presented here provide a much greater understanding of the full annual-cycle of the Great Knots which spend the seven month long non-breeding season at Roebuck Bay in north-west Australia. Migration, which covered approx. 20,000 km for the round trip, typically took up to 3.5 months of the remaining time. The geolocators revealed the migration strategy employed, including making small stops before arriving at the principal stopovers in the Yellow Sea on both northward and southward migrations. Arrival at the breeding grounds and the laying of eggs were remarkably synchronous between individuals, as were the arrival dates back at Roebuck Bay. Departure from the breeding

grounds was more spread out, partly dependent on breeding success and probably also as a result of females leaving the nesting area before males (Tomkovich 1997). Overall, the results indicate the tight schedules into which shorebirds must fit their annual cycle, the strong dependency on crucial refuelling sites along their journey, and that ongoing degradation in the Yellow Sea will likely have further negative effects on the Great Knot population.

ACKNOWLEDGEMENTS

ONLINE SUPPLEMENTARY MATERIAL

DOI: 10.18194/ws.00048

S1. Incubation and brooding patterns

S2. Migration paths (MCMC estimates)

S3. Individual migration schedules

REFERENCES

Antonov, A. & F. Huettman. 2008. Observation of shorebirds during southward migration at Schastia Bay, Sea of Okhotsk, Russia: July, 23 – August 8 2006 and July, 25 – August, 1 2007. *Stilt* 54: 13–18.

Barter, M.A. 2002. *Shorebirds of the Yellow Sea: importance, threats and conservation status.* International Wader Studies No. 12 and Wetlands International Global Series No. 9, Wetlands International – Oceania, Canberra, Australia.

Barter, M., D. Tonkinson, T. Sixian, Y. Xiao & Q. Fawen. 1997. Staging of the Great Knot *Calidris tenuirostris*, Red

Knot *C. canutus* and Bar-tailed Godwit *Limosa lapponica* at Chongming Dao, Shanghai: Jumpers to hoppers? *Stilt* 31: 2–11.

Battley, P.F., T. Piersma, M.W. Dietz, S.X. Tang, A. Dekinga & K. Hulsman. 2000. Empirical evidence for differential organ reductions during trans-oceanic bird flight. *Proceedings of the Royal Society B: Biological Sciences* 267: 191–195.

Battley, P.F., N. Warnock, T.L. Tibbitts, R.E. Gill, T. Piersma, C.J. Hassell, D.C. Douglas, D.M. Mulcahy, B.D. Gartrell, R. Schuckard, D.S. Melville & A.C. Riegen. 2012. Contrasting extreme long-distance migration patterns in bar-tailed godwits *Limosa lapponica*. *Journal of Avian Biology* 43: 21–32.

Burger, J., L.J. Niles, R.R. Porter & A.D. Dey. 2012. Using geolocator data to reveal incubation periods and breeding biology in Red Knots *Calidris canutus rufa*. *Wader Study Group Bulletin* 119: 26–36.

Clemens, R.S., D.I. Rogers, B.D. Hansen, K. Gosbell, C.D.T. Minton & 17 others. 2016. Continental-scale decreases in shorebird populations in Australia. *Emu* 116: 119–135.

Delany, S. & D. Scott. 2006. *Waterbird population estimates. 4th Edition.* Wetlands International, Wageningen, The Netherlands.

Gerasimov, Y., Y. Artukhin, N. Gerasimov & N. Lobkov. 1999. Status of shorebirds in Kamchatka, Russia. *Stilt* 34: 31–34.

Gerasimov, Y. & N.N. Gerasimov. 2000. The importance of the Moroschechnya River Estuary as a staging site for shorebirds. *Stilt* 36: 20–25.

Gosbell, K., C. Minton & J. Fox. 2012. Geolocators reveal incubation and re-nesting characteristics of Ruddy Turnstones *Arenaria interpres* and Eastern Curlews *Numenius madagascariensis*. *Wader Study Group Bulletin* 119: 160–171.

Hansen, B.D., R.A. Fuller, D. Watkins, D.I. Rogers, R.S. Clemens, M. Newman, E.J. Woehler & D.R. Weller. 2016. *Revision of the East Asian-Australasian Flyway Population Estimates for 37 listed Migratory Shorebird Species.* Department of the Environment, BirdLife Australia, Melbourne.

Higgins, P.J. & S.J.J.F. Davies. 1996. *Handbook of Australian, New Zealand and Antarctic birds.* Oxford University Press, Melbourne, Australia.

Huettmann, F. 2001. Summary of a trip to the Sea of Okhotsk to study migrating shorebirds: May 2000 on southern Sakhalin Island and August 2000 on western Kamchatka and Magadan region. *Stilt* 39: 65–71.

Huettmann, F. 2003. Shorebird migration on northern Sakhalin Island, Russia in early northern autumn 2002. *Stilt* 43: 34–39.

Lane, B.A. 1987. *Shorebirds in Australia.* Nelson Publishers, Melbourne, Australia.

Lappo, E., P.S. Tomkovich & E. Syroechkovskiy. 2012. *Atlas of Breeding Waders in the Russian Arctic.* UF Ofsetnaya Pechat, Moscow.

Lisovski, S., K. Gosbell, M. Christie, B.J. Hoye, M.

Klaassen, I.D. Stewart, A.J. Taysom & C. Minton. 2016. Movement patterns of Sanderling (*Calidris alba*) in the East Asian–Australasian Flyway and a comparison of methods for identification of crucial areas for conservation. *Emu* 116: 168–177.

Lisovski, S. & S. Hahn. 2012. GeoLight – processing and analysing light-based geolocator data in R. *Methods in Ecology & Evolution* 3: 1055–1059.

Lisovski, S., C.M. Hewson, R.H.G. Klaassen, F. Korner-Nievergelt, M.W. Kristensen & S. Hahn. 2012. Geolocation by light: accuracy and precision affected by environmental factors. *Methods in Ecology & Evolution* 3: 603–612.

Loktionov, E.Y., P.S. Tomkovich & R.R. Porter. 2016. Study of incubation, chick rearing and breeding phenology of Red Knots *Calidris canutus rogersi* in sub-Arctic Far Eastern Russia aided by geolocators. *Wader Study* 122: 142–152.

Ma, Z.J., N. Hua, H.B. Peng, C. Choi, P.F. Battley, Q.Y. Zhou, Y. Chen, Q. Ma, N. Jia, W.J. Xue, Q.Q. Bai, W. Wu, X.S. Feng & C.D. Tang. 2013. Differentiating between stopover and staging sites: functions of the southern and northern Yellow Sea for long-distance migratory shorebirds. *Journal of Avian Biology* 44: 504–512.

Ma, Z.J., D.S. Melville, J.G. Liu, Y. Chen, H.Y. Yang, W.W. Ren, Z.W. Zhang, T. Piersma & B. Li. 2014. Rethinking China's new great wall. *Science* 346: 912–914.

Minton, C., K. Gosbell, P. Johns, M. Christie, M. Klaassen, C. Hassell, A. Boyle, R. Jessop & J. Fox. 2013. New insights from geolocators deployed on waders in Australia. *Wader Study Group Bulletin* 120: 37–46.

Minton, C., J. Wahl, H. Gibbs, R. Jessop, C. Hassell & A. Boyle. 2011. Recoveries and flag sightings of waders which spend the non-breeding season in Australia. *Stilt* 50: 17–43.

Moores, N., D.I. Rogers, K. Rogers & P.M. Hansbro. 2016. Reclamation of tidal flats and shorebird declines in Saemangeum and elsewhere in the Republic of Korea. *Emu* 116: 136–146.

Murray, N.J., R.S. Clemens, S.R. Phinn, H.P. Possingham & R.A. Fuller. 2014. Tracking the rapid loss of tidal wetlands in the Yellow Sea. *Frontiers in Ecology & the Environment* 12: 267–272.

Pennycuick, C.J., S. Åkesson & A. Hedenström. 2013. Air speeds of migrating birds observed by ornithodolite and compared with predictions from flight theory. *Journal of the Royal Society Interface* 10: 20130419.

Piersma, T. 1987. Hop, skip or jump? Constraints on migration of Arctic waders by feeding, fattening, and flight speed. *Limosa* 60: 185–194. [In Dutch]

Piersma, T., T. Lok, Y. Chen, C.J. Hassell, H.Y. Yang, A. Boyle, M. Slaymaker, Y.C. Chan, D.S. Melville, Z.W. Zhang & Z.J. Ma. 2016. Simultaneous declines in summer survival of three shorebird species signals a flyway at risk. *Journal of Applied Ecology* 53: 479–490.

Rogers, D., K. Rogers, K. Gosbell & C. Hassell. 2007. Causes of variation in population monitoring surveys: insights from non-breeding counts in north-western Australia. *Stilt* 50: 176–193.

Summers, R.W., L.G. Underhill & R. Prys-Jones. 1995. Why do young waders in southern Africa delay their first return migration to the breeding ground. *Ardea* 83: 351–357.

Sumner, M.D., S.J. Wotherspoon & M.A. Hindell. 2009. Bayesian estimation of animal novement from archival and satellite tags. *PLoS One* 4: e7324.

Tomkovich, P.S. 1997. Breeding distribution, migrations and conservation status of the great knot *Calidris tenuirostris* in Russia. *Emu* 97: 265–282.

Tomkovich, P.S. 2003. List of wader species of Chukotka, northern far east of Russia: Their banding and migratory links. *Stilt* 44: 29–43.

Venables, W.N. & B.D. Ripley. 2002. *Modern Applied Statistics with S.* Springer, New York.

Warnock, N. 2010. Stopping vs. staging: the difference between a hop and a jump. *Journal of Avian Biology* 41: 621–626.

Weiser, E.L., R.B. Lanctot, S.C. Brown, J.A. Alves, P.F. Battley & 45 others. 2016. Effects of geolocators on hatching success, return rates, breeding movements, and change in body mass in 16 species of Arctic-breeding shorebirds. *Movement Ecology* 4: 12.

Williams, T.C. & J.M. Williams. 1988. Radar and visual observations of autumnal (southward) shorebird migration on Guam. *Auk* 105: 460–466.

Wotherspoon, S.J., D.A. Sumner & S. Lisovski. 2013. *R Package SGAT: Solar/Satellite Geolocation for Animal Tracking.* GitHub. Accessed at: *https://github.com/SWotherspoon/ SGAT*